



UNIVERSITY OF LEEDS

This is a repository copy of *Inhibiting ABCG2 could potentially enhance the efficacy of hypericin-mediated photodynamic therapy in spheroidal cell models of colorectal cancer.*

White Rose Research Online URL for this paper:
<http://eprints.whiterose.ac.uk/134100/>

Version: Accepted Version

Article:

Khot, MI, Perry, SL orcid.org/0000-0002-2561-8195, Maisey, T et al. (5 more authors) (2018) Inhibiting ABCG2 could potentially enhance the efficacy of hypericin-mediated photodynamic therapy in spheroidal cell models of colorectal cancer. *Photodiagnosis and Photodynamic Therapy*, 23. pp. 221-229. ISSN 1572-1000

<https://doi.org/10.1016/j.pdpdt.2018.06.027>

© 2018 Elsevier B.V. This manuscript version is made available under the CC-BY-NC-ND 4.0 license <http://creativecommons.org/licenses/by-nc-nd/4.0/>.

Reuse

This article is distributed under the terms of the Creative Commons Attribution-NonCommercial-NoDerivs (CC BY-NC-ND) licence. This licence only allows you to download this work and share it with others as long as you credit the authors, but you can't change the article in any way or use it commercially. More information and the full terms of the licence here: <https://creativecommons.org/licenses/>

Takedown

If you consider content in White Rose Research Online to be in breach of UK law, please notify us by emailing eprints@whiterose.ac.uk including the URL of the record and the reason for the withdrawal request.



eprints@whiterose.ac.uk
<https://eprints.whiterose.ac.uk/>

Inhibiting ABCG2 could potentially enhance the efficacy of Hypericin-mediated photodynamic therapy in spheroidal cell models of colorectal cancer

M. Ibrahim Khot^{*,1}, Sarah L. Perry¹, Thomas Maisey¹,
Gemma Armstrong¹, Helen Andrew¹, Thomas A. Hughes¹,
Nikil Kapur² and David G. Jayne¹

1. School of Medicine, St. James's University Hospital, University of Leeds, Beckett St., Leeds, LS9 7TF, UK
2. School of Mechanical Engineering, University of Leeds, Leeds, LS2 9JT, UK

*Corresponding author: M. Ibrahim Khot

Email: ummik@leeds.ac.uk

Address: Section of Translational Anaesthesia and Surgical Sciences,
Level 9, Wellcome Trust Brenner Building,
St. James's University Hospital, University of Leeds,
Beckett St., Leeds,
LS9 7TF, UK

ABSTRACT

Background: Photodynamic Therapy (PDT) is an attractive modality for treating solid cancers. This study evaluates the efficacy of Hypericin-PDT as a cytotoxic therapy in colorectal cancer (CRC), using 2D cell cultures and 3D multicellular tumour spheroids.

Methods: Spheroids were generated through forced-floating and agitation-based techniques. 2D and spheroid models of HT29 and HCT116 CRC cells were incubated with Hypericin (0–200nM) for 16 hours. Cultures were irradiated with light ($1\text{J}/\text{cm}^2$) and cytotoxicity assessed using Propidium Iodide fluorescence. Expression of ABCG2 protein was assessed by immunoassays in 2D and spheroid cultures. The effect of ABCG2 inhibition, using $10\mu\text{M}$ Ko143, on cytotoxicity following Hypericin-PDT was evaluated.

Results: Hypericin-PDT produced a significant reduction in HT29 ($p<0.0001$) and HCT116 ($p<0.0001$) cell viability in 2D cultures, with negligible non-phototoxicity. Spheroids were more resistant than 2D cultures to Hypericin-PDT (HT29: $p=0.003$, HCT116: $p=0.006$) and had a greater expression of ABCG2. Inhibition of ABCG2 in spheroids with Ko143 resulted in an enhanced Hypericin-PDT effect compared to Hypericin-PDT alone (HT29: $p=0.04$, HCT116: $p=0.01$).

Conclusions: Hypericin-PDT has reduced efficacy in CRC spheroids as compared to 2D cultures, which maybe attributable through upregulation in ABCG2. The clinical efficacy of Hypericin-PDT maybe enhanced by ABCG2 inhibition.

Keywords: Colorectal cancer, Hypericin, Photodynamic Therapy, ABCG2,
Multicellular Tumour Spheroids, Ko143

INTRODUCTION

Photodynamic Therapy (PDT) involves the administration of a tumour-retaining photosensitiser (PS), followed by light administration to generate reactive oxygen species (ROS) that cause necrosis and apoptosis, depending on the type and concentration of PS, light dose and tissue sensitivity [1–3]. Hypericin, a photoactive compound found in St. John's Wort (*Hypericum perforatum*) [4], has attracted interest through its diverse range of medicinal applications, including PDT in pre-clinical cancer studies [5–12]. Hypericin possesses several advantages over other photosensitisers, including a wide light absorption spectrum, low photobleaching, high quantum yield and negligible non-phototoxicity [8,13–15].

Pre-clinical evaluation of anti-cancer therapeutics has traditionally used two-dimensional (2D) monolayer cancer cell cultures, which are simple and reliable. However, they fail to replicate the diversity and complexity of *in vivo* cancers [16,17]. Solid tumours exhibit heterogeneity in access to oxygen, nutrients and essential growth factors leading to diversity in intra-tumoural cellular proliferation, survival and response to anti-cancer treatment [18], which cannot be reproduced in 2D cell cultures [19,20]. Three-dimensional (3D) multicellular tumour spheroids simulate a more realistic *in vivo* cancer model [21] incorporating the cellular interactions that are crucial to signalling pathways, and the heterogeneous distribution of oxygen and metabolites that influence proliferation and survival [22,23]. Spheroids also provide useful information on the spatiotemporal distribution and pharmacokinetics of anti-cancer drugs [24].

Chemotherapy is routinely given post-operatively to colorectal cancer (CRC) patients at high-risk of recurrence, but with a survival advantage of only 10% [25,26]. Alternative treatment strategies are therefore required to improve outcomes. PDT is one such strategy, supported by clinical evidence of efficacy: the outcome for patients with lung [27] and bladder [28] cancers has been shown to be improved by the addition of PDT as compared to surgery alone. PDT also has a role in palliation and does not interact with other adjuvant therapy [29].

The aim of the current investigation is to compare the efficacy of Hypericin-PDT in 2D and spheroid CRC cultures and to explain any differences observed in terms of the cellular characteristics of the two models.

MATERIALS AND METHODS

Materials

Hypericin was obtained from Molecular Probes® by Life Technologies™ (Eugene, Oregon, USA) and prepared as a 100µM stock solution in ethanol. 1mL aliquots of the stock solution was stored in the dark. Ko143 hydrate, an inhibitor of ABCG2, was purchased from Sigma Aldrich (Gillingham, UK) and was prepared as a 1mg/mL stock solution in DMSO and stored as 100µL aliquots.

Cell line and culturing conditions

Human colon cancer cell lines, HCT116 and HT29, were obtained from the European Collection of Authenticated Cell Cultures (Salisbury, UK). Both cell lines were cultured in Roswell Park Memorial Institute (RPMI) 1640 Medium plus GlutaMAX™ (Gibco® by Life Technologies™, Paisley, UK) supplemented with 10% (v/v) Fetal Bovine Serum (FBS) (Sigma-Aldrich). Cell cultures were maintained at 37°C/5% CO₂/95% relative humidity. Upon 80-90% confluency, cell cultures were washed with Dulbecco's Phosphate-Buffered Saline (DPBS, Gibco® by Life Technologies™) and incubated for 5 minutes with 0.05% (v/v) trypsin and 0.5% (v/v) ethylenediaminetetraacetic acid (EDTA, Gibco® by Life Technologies™) in DPBS. Cell medium containing 10% (v/v) FBS was added to trypsinised cells and the cell suspensions centrifuged at 400g for 5 minutes. The supernatant was discarded and the pelleted cells resuspended in fresh medium, seeded into 75cm² tissue culture flasks (Corning Inc., New York, USA) and grown to 80-90% confluence for the experiments.

Photodynamic therapy

For 2D cell cultures, 5×10^4 cells were seeded per well into 96-well tissue culture plates (Corning Inc.) and incubated at $37^\circ\text{C}/5\% \text{CO}_2/95\%$ for 24 hours. For spheroid cultures, agarose powder (Sigma-Aldrich) was dissolved into deionised water to make a 1% solution. $50\mu\text{L}$ of the agarose solution was added into each well of a 96-well plate, and left at room temperature for 20 minutes to gel. 500 cells were then added to each well and the plate centrifuged at $360g$ for 10 minutes and incubated at $37^\circ\text{C}/5\% \text{CO}_2/95\%$ for 48 hours. Cell cultures were treated with (0-200nM) Hypericin in the dark for 16 hours before being washed with DPBS. Phenol red-free RPMI 1640 medium with L-glutamine (Gibco® by Life Technologies™) supplemented with 10% (v/v) FBS was added to cultures. Depending on the experimental conditions, cultures were either irradiated with light or kept in the dark at room temperature.

Light treatment

Cell culture plates were placed on top of the diffuser surface of a light-radiating device and treated with a light dose of $1\text{J}/\text{cm}^2$. Light treatment lasted for 72 minutes and 28 seconds at $0.23\text{mW}/\text{cm}^2$. The light-radiating device comprised of a series of LED's (one hundred and ninety-two HLMP-EL3B-WXKDD Amber LEDs (Avago Technologies, California, USA), with peak wavelength of 594nm and a spectral half-width of 13nm, and an internal fan to prevent overheating.

Inhibiting ABCG2

Cell cultures were incubated with $10\mu\text{M}$ Ko143 at $37^\circ\text{C}/5\% \text{CO}_2/95\%$ for 90 minutes followed by the addition of increasing doses of Hypericin (0 – 200nM) for

an additional 16 hours. Cultures were then washed and treated with light as described above.

Assessing Cell Viability

Quantifying cytotoxicity: Twenty-four hours following irradiation, 2D and spheroid cultures were treated with 1.3µg/mL propidium iodide (Biotium Inc., California, USA) for 15 minutes. Cell cultures were then washed twice with DPBS and fresh cell culture medium added. Fluorescence was measured on a Mithras LB 940 Microplate Reader (Ex: 540nm, Em: 620nm) (Berthold Technologies Ltd., Harpenden, UK).

Visualising cytotoxicity: Twenty-four hours following irradiation, spheroid cultures were incubated with 1.3µg/mL propidium iodide (excitation: 530nm, emission: 620nm, exposure time: 500ms) and 5µg/mL Hoechst 33342 (excitation: 350nm, emission: 450nm, exposure time: 500ms) (Life Technologies™) simultaneously for 15 and 60 minutes respectively. spheroids were then washed and fluorescence visualised using the EVOS™ FL Imaging System (Life Technologies™).

Spinner flask spheroid culture

Cells were washed and trypsinised and the cell suspensions transferred into CELLSPIN Stirrer spinner flasks (INTEGRA Biosciences Corp., New Hampshire, USA), where they were maintained in cell culture medium with constant agitation at 75 rpm on a stirring platform and incubated at 37°C/5% CO₂/95%. Cell culture media was changed every 3 days. Fifteen to twenty day old spheroids were used for experiments.

Immunofluorescence staining

Spinner flask spheroids were embedded into Cryo-M-bed (Bright Instruments, Luton, UK) and sections (5µm) were cut onto glass slides using a Leica CM3050 S Research Cryostat (Leica Microsystems (UK) Ltd, Milton Keynes, UK). 2D cultures were grown to confluency on glass coverslips. Spheroid sections and 2D cultures were fixed with 4% PFA, blocked with 0.5% skimmed milk and incubated with anti-BCRP antibody (1:20, BXP-21) (Millipore, Watford, UK) for 1 hour at room temperature. They were then washed with PBS and incubated with an Alexa Fluor 488-conjugated secondary antibody (1:300) (Life Technologies™) for 30 minutes at room temperature. Slides and coverslips were washed and mounted using ProLong™ Gold Antifade Mountant with DAPI (Life Technologies™). Slides were imaged using the Zeiss Axio Imager Z1 (Carl Zeiss Ltd, Cambridge, UK).

Protein extraction and Western blotting

Spinner flask spheroids were washed with ice-cold DPBS and sonicated in RIPA buffer with protease inhibitor for 15 minutes. Similarly, 2D cultures were grown to confluency in a 75cm² cell-culturing flask, washed with ice-cold DPBS, and lysed in RIPA buffer with protease inhibitor for 15 minutes. Lysed cells were centrifuged at 14,000 rpm for 10 minutes and the supernatant was aliquoted and stored at -80°C. Protein concentration was determined using the DC™ Protein Assay kit (Bio-Rad, Watford, UK). Lysates were resolved using LDS-PAGE and blotted onto a PVDF Transfer Membrane (Thermo Fisher Scientific, Altrincham, UK). The membranes were blocked with 5% skimmed milk for 30 minutes, followed by further blocking with 1% skimmed milk for an additional 30 minutes. The membranes were incubated overnight at 4°C with an anti-BCRP antibody

(1:200, BXP-21) (Millipore, Watford, UK). The membranes were then incubated with a horseradish peroxidase-conjugated secondary antibody for 1 hour at room temperature prior to developing bands using the SuperSignal™ West Femto Maximum Sensitivity Substrate (Thermo Fisher Scientific) and imaged on the ChemiDoc™ XRS+ System (Bio-Rad). β -actin served as a loading control.

Uptake of Hypericin in spheroids

Spinner flask spheroids were treated with 200nM Hypericin for 16 hours, embedded, sectioned onto slides and mounted as described above. Slides were imaged on the Nikon A1R Confocal Microscope (Nikon UK Ltd, Kingston upon Thames, UK).

Prolonged culture of spheroids following Ko143 treatment and Hypericin-PDT

Spheroids were grown in agarose-coated plates, then subjected to Ko143 incubation and Hypericin-PDT as described above. Spheroids were cultured for an additional 10 days with cell culture media changed every day. Transillumination images of spheroids were taken using the EVOS™ FL Imaging System. Volumes of spheroids were calculated using ImageJ (National Institutes of Health, Maryland, USA).

Statistical Analysis

One-way ANOVA and Student's *t*-test were used to perform statistical analysis using GraphPad Prism 7 (GraphPad Software, Inc., California, USA). $p < 0.05$ was considered to be statistically significant. Data are presented as the mean \pm standard deviation.

RESULTS

Photoactivation of Hypericin

Hypericin treated cells stimulated with light exhibited a significant dose dependant reduction in cell viability as compared to untreated controls (100nM Hypericin: HT29 38% cell viability, $p=0.0001$ and HCT116 34% cell viability, $p<0.0001$), whilst control cultures kept in the dark failed to show any response to treatment (100nM Hypericin: HT29 99% cell viability, $p=0.33$ and HCT116 99% cell viability, $p=0.18$) (Figure 1A and 1B). A similar result was observed when HT29 and HCT116 spheroids were subjected to Hypericin-mediated PDT, as indicated by increasing propidium iodide fluorescence, which was not apparent in control spheroids kept in the dark (Figure 1C).

2D vs. 3D response to Hypericin-PDT

Both HT29 and HCT116 spheroids were significantly more resistant to Hypericin mediated PDT induced cell death as compared to their respective monolayer cell cultures. (100nM Hypericin: HT29 spheroids 35% more viable, $p<0.0001$ and HCT116 spheroids are 32% more viable, $p=0.01$) (Figure 2A & 2B).

Expression of the ABCG2 protein

The ABCG2 transmembrane associated protein was observed in both HT29 and HCT116 cell lines in 2D cultures, as assessed by immunofluorescence (Figures 3A & 3B). Figures 3C and 3D illustrate the distribution of ABCG2 protein expression in HT29 and HCT116 spheroids respectively. The protein expression

of ABCG2 was most prominent in the outer layers of cells, whereas the core of the spheroid had lower levels of expression. On western blot analysis, the protein expression of ABCG2 was lower in HCT116 as compared to HT29 2D cultures (Figure 3C). There was a significant reduction in ABCG2 protein expression in 2D as compared to spheroid cultures for both HT29 and HCT116 (Figure 3E & 3F). Similar to 2D cultures, HCT116 demonstrated lower expression of ABCG2 protein as compared to HT29 in spheroid cultures.

ABCG2 mediated resistance to Hypericin-PDT

Figures 4A and 4B show 2D cultures of HT29 and HCT116 cells co-treated with 10 μ M Ko143 (ABCG2 inhibitor) and Hypericin-PDT or Hypericin-PDT alone. A significant difference in cell viability was observed in 2D HT29 cells co-treated with Ko143 and Hypericin-PDT compared to Hypericin-PDT only treated cells (10nM Hypericin: 38% decrease in cell viability, $p=0.02$). With increasing concentrations of Hypericin, the Ko143 co-treated 2D HT29 cells showed a dose dependent decrease in cell viability. However, at the higher concentrations of Hypericin, there was no difference between the co-treated and Hypericin-PDT only cultures (Figure 4A). In 2D HCT116 cultures, no significant difference in cell viability was observed between Ko143 treated and untreated samples subjected to Hypericin-PDT ($p=0.94$) (Figure 4B). In spheroid models of both HT29 and HCT116 cell lines, a significant difference in cell viability was observed between Ko143 and Hypericin-PDT co-treated and Hypericin-PDT alone cell cultures (100nM Hypericin: HT29 spheroids 11% less viable, $p=0.01$ and HCT116 spheroids 9% less viable, $p=0.02$) (Figure 4C & 4D). Unlike 2D cultures, the

effect of Ko143 on both HT29 and HCT116 spheroid viability was still apparent at higher doses of Hypericin-PDT.

Penetration of Hypericin in CRC spheroids

Hypericin penetrated through to the central core of both HT29 and HCT116 spheroids (Figure 5A and 5B). The penetration of Hypericin through the spheroids corresponds with the expression of ABCG2 protein. A higher ABCG2 protein expression in the thicker peripheral layers of proliferating cells in HT29 spheroids was observed, as compared to HCT116 spheroids (Figure 3C and 3D), and may have amounted to the lower retention of Hypericin in the peripheral cell layers of HT29 spheroids as compared to HCT116 spheroids (Figure 5).

Re-growth of spheroids following ABCG2 inhibition and Hypericin-PDT

Twenty-four hours following ABCG2 inhibition and Hypericin-PDT, HT29 and HCT116 spheroids had lost their compact spheroidal integrity as indicated by the loose cellular debris and loss of structure (Figure 6C). By day 4, spheroids had begun to re-form their shapes and continued to increase in volume. By day 10, Ko143 and 200nM Hypericin co-treated spheroids were significantly larger as compared to the sizes of spheroids on day 0. (HT29 spheroids: 0.22mm³ increased volume, $p < 0.005$ and HCT116 spheroids: 0.44mm³ increased volume, $p < 0.02$) (Figure 6A & 6B).

DISCUSSION

Photodynamic therapy is an attractive treatment for solid cancers, which can be combined with other therapies and serve as an adjunct to surgical excision [29,30]. The clinical application of the first generation of photosensitisers

was hampered by unwanted adverse effects, notably photohypersensitivity reactions and non-light toxicities [31]. In comparison, Hypericin possesses negligible dark toxicity, yet retains a potent phototoxicity, giving it a beneficial therapeutic index.

Many anti-cancer drugs that have shown promise *in vitro* have subsequently failed to achieve their potential in clinical studies. Some of this is attributable to the methods used in pre-clinical evaluation. Traditional 2D culture models are simplistic representations of cancers *in vivo* and can give misleading results about drug efficacy. In comparison, 3D spheroids are recognised to be better models of cancers *in vivo* and have previously been shown to be useful in PDT related studies [32]. Generally, 3D spheroids are more resistant to anti-cancer treatments, including PDT, as compared to 2D cultures [23,33]. These findings have been corroborated by our results as well as other studies assessing Hypericin-PDT in 2D and 3D cell cultures [34]. Yang *et al.* also reported an increased resistant to PDT in 3D cultures as compared to 2D models of breast cancer when challenged with 5-ALA mediated PDT [35]. Unlike 2D cell cultures, where the exposure to PS and light is uniform, the spherical structure of spheroids influences the diffusion of the PS and penetration of radiating light. This produces a diminishing gradient of PS and light towards the core of the 3D structure, simulating *in vivo* conditions, which, in combination with decreasing oxygen tensions, limits the PDT effect in the centre of the spheroid. 3D *in vitro* cancer models therefore fill an essential gap between simple monolayer cell cultures and resource intensive and expensive animal models for pre-clinical drug evaluation [35].

The breast cancer resistance protein also known as ABCG2, is a well-known member of the ATP-binding cassette (ABC) transporter superfamily [36]. It plays a vital role in the uptake, distribution and elimination of xenobiotics and other metabolites. ABCG2 has been documented to be over-expressed in various cancer cell lines, and can confer resistance to various chemotherapeutics by mediating the ATP-dependent efflux of compounds from cells [37,38]. We have demonstrated the expression of ABCG2 protein in CRC cell models with an upregulation in spheroids, suggesting that adaptive cell signalling pathways exist in cancer cells to promote survival [39]. Additionally, we have shown that the protein expression of ABCG2 is higher in the outer layers of spheroids as compared to the inner and central areas (Figure 3C and 3D). The non-uniformed expression of ABCG2 protein in spheroids highlights the physiological advantage they possess in providing a better *in vitro* platform for anti-cancer evaluations. The relevance of our *in vitro* findings to the clinical scenario is evidenced in the work of Liu *et al.* who found ABCG2 to be highly expressed in human colorectal cancers as compared to low expression in non-cancer tissue [40].

Previous studies have shown a correlation between high expression levels of ABCG2, low intracellular accumulation of PS and limited PDT effect [41–43]. Jendzelovsky *et al.* identified Hypericin as a preferential substrate for ABCG2 [44]. When HT29 cells were treated with Hypericin, they showed an increased expression in ABCG2 compared to untreated cells, whilst inhibition of ABCG2 increased the intracellular Hypericin levels. The effect of ABCG2 inhibition on intracellular Hypericin accumulation has also been confirmed by others [45]. Furthermore, ABCG2 has been implicated in playing a protective role against ROS mediated toxicity [46,47]. It therefore appears that ABCG2 is an important

mediator of the efficacy of Hypericin-PDT. Our studies have confirmed this in CRC models, demonstrating an additive cytotoxic effect when Hypericin-PDT is combined with Ko143 inhibition of ABCG2. Similar findings have also been reported by others in 2D cultures of oesophageal, bladder, breast, glioblastoma and colorectal cancers cell lines [41,48–50].

We have observed the diffusion of Hypericin through to the core of the spheroid models. However, only ~40-50% spheroid cellular death was achieved at the highest concentration of Hypericin, when both HT29 and HCT116 spheroids were co-treated with Hypericin-PDT and Ko143. Oxygen tensions are known to vary in spheroids, with decreasing gradients from the outer layers to the hypoxic core [51,52]. It is possible that the lack of oxygen in the core could have been a limiting factor to the overall cytotoxic effects of PDT in spheroids.

To further highlight the clinical relevance of evaluating PDT in spheroids, we observed that both HT29 and HCT116 spheroids had begun to regrow and reform their shapes by day 4 after Hypericin-PDT. This highlights the need for repeat application of PDT in order to control malignant proliferation and achieve effective cancer killing. Such strategies have been developed through the use of low dose fractionated PDT, which appears to be more efficacious than single dose PDT application [53,54].

In summary, our studies add to the evidence base about the potential application of Hypericin-PDT as an anti-cancer strategy in CRC. We have shown that 3D spheroid models of CRC are more resistant to Hypericin-PDT as compared to 2D models, which can be overcome, to some extent, by specific

inhibition of the ABCG2 transporter. Further research is required to confirm these findings in pre-clinical small animal models, but our initial findings offer an exciting insight into new strategies for enhancing PDT efficacy in CRC.

DECLARATIONS OF INTEREST: NONE

FUNDING

University of Leeds 110 Anniversary Research Scholarships

REFERENCES

- [1] D.E.J.G.J. Dolmans, D. Fukumura, R.K. Jain, Photodynamic therapy for cancer., *Nat. Rev. Cancer.* 3 (2003) 380–7. doi:10.1038/nrc1071.
- [2] T.J. Dougherty, C.J. Gomer, B.W. Henderson, G. Jori, D. Kessel, M. Korblick, J. Moan, Q. Peng, Photodynamic therapy., *J. Natl. Cancer Inst.* 90 (1998) 889–905.
<http://www.ncbi.nlm.nih.gov/pubmed/9637138>.
- [3] P. Agostinis, K. Berg, K.. Cengel, T.. Foster, A.. Girotti, S.. Gollnick, S.. Hahn, M.. Hamblin, A. Juzeniene, D. Kessel, M. Koberlik, J. Moan, P. Mroz, D. Nowis, J. Piette, B. Wilson, J. Golab, Photodynamic Therapy of cancer: an update, *CA Cancer J Clin.* 61 (2011) 250–281.
doi:10.3322/caac.20114.PHOTODYNAMIC.
- [4] S.L. Crockett, N.K.B. Robson, Taxonomy and Chemotaxonomy of the Genus *Hypericum*., *Med. Aromat. Plant Sci. Biotechnol.* 5 (2011) 1–13. <http://www.ncbi.nlm.nih.gov/pubmed/22662019>.
- [5] P. Agostinis, A. Vantieghe, W. Merlevede, P.A.M. De Witte, Hypericin in cancer treatment: More light on the way, *Int. J. Biochem. Cell Biol.* 34 (2002) 221–241. doi:10.1016/S1357-2725(01)00126-1.
- [6] K. Maduray, L. Davids, The Anticancer Activity of Hypericin in Photodynamic Therapy, *J. Bioanal. Biomed.* s6 (2011) 4–6. doi:10.4172/1948-593X.S6-004.

- [7] A. Kubin, F. Wierrani, U. Burner, G. Alth, W. Grunberger, Hypericin - The Facts About a Controversial Agent, *Curr. Pharm. Des.* 11 (2005) 233–253. doi:10.2174/1381612053382287.
- [8] Y. Xu, D. Wang, Z. Zhuang, K. Jin, L. Zheng, Q. Yang, K. Guo, Hypericin-mediated photodynamic therapy induces apoptosis in K562 human leukemia cells through JNK pathway modulation, *Mol. Med. Rep.* 12 (2015) 6475–6482. doi:10.3892/mmr.2015.4258.
- [9] V. Sacková, P. Fedorocko, B. Szilárdiová, J. Mikes, J. Kleban, Hypericin-induced photocytotoxicity is connected with G2/M arrest in HT-29 and S-phase arrest in U937 cells., *Photochem. Photobiol.* 82 (2006) 1285–91. doi:10.1562/2006-02-22-RA-806.
- [10] J. Mikes, J. Kleban, V. Sacková, V. Horváth, E. Jamborová, A. Vaculová, A. Kozubík, J. Hofmanová, P. Fedorocko, Necrosis predominates in the cell death of human colon adenocarcinoma HT-29 cells treated under variable conditions of photodynamic therapy with hypericin., *Photochem. Photobiol. Sci.* 6 (2007) 758–66. doi:10.1039/b700350a.
- [11] B. Kleemann, B. Loos, T.J. Scriba, D. Lang, L.M. Davids, St John's Wort (*Hypericum perforatum* L.) photomedicine: Hypericin-photodynamic therapy induces metastatic melanoma cell death, *PLoS One.* 9 (2014). doi:10.1371/journal.pone.0103762.
- [12] L. Balogová, M. Maslaňáková, L. Dzurová, P. Miškovský, K. Stroffeková, Bcl-2 proapoptotic proteins distribution in U-87 MG glioma cells before and after hypericin photodynamic action., *Gen. Physiol. Biophys.* 32 (2013) 179–87. doi:10.4149/gpb_2013021.
- [13] A.M. Lima, C.D. Pizzol, F.B.F. Monteiro, T.B. Creczynski-Pasa, G.P. Andrade, A.O. Ribeiro, J.R. Perussi, Hypericin encapsulated in solid lipid nanoparticles: Phototoxicity and photodynamic efficiency, *J. Photochem. Photobiol. B Biol.* 125 (2013) 146–154. doi:10.1016/j.jphotobiol.2013.05.010.
- [14] B. Ehrenberg, J.L. Anderson, C.S. Foote, Kinetics and Yield of Singlet Oxygen Photosensitized by Hypericin in Organic and Biological Media, *Photochem. Photobiol.* 68 (1998) 135–140. doi:10.1111/j.1751-1097.1998.tb02479.x.
- [15] R. Ritz, C. Scheidle, S. Noell, F. Roser, M. Schenk, K. Dietz, W.S.L. Strauss, In Vitro Comparison of Hypericin and 5-Aminolevulinic Acid-Derived Protoporphyrin IX for Photodynamic Inactivation of Medulloblastoma Cells, *PLoS One.* 7 (2012) 1–11. doi:10.1371/journal.pone.0051974.
- [16] A.A. Salahudeen, C.J. Kuo, Toward recreating colon cancer in human organoids, *Nat. Med.* 21 (2015)

215–216. doi:10.1038/nm.3818.

- [17] M. Vinci, S. Gowan, F. Boxall, L. Patterson, M. Zimmermann, W. Court, C. Lomas, M. Mendiola, D. Hardisson, S.A. Eccles, Advances in establishment and analysis of three-dimensional tumor spheroid-based functional assays for target validation and drug evaluation, *BMC Biol.* 10 (2012) 29. doi:10.1186/1741-7007-10-29.
- [18] L.-B. Weiswald, S. Richon, P. Validire, M. Briffod, R. Lai-Kuen, F.P. Cordelières, F. Bertrand, D. Dargere, G. Massonnet, E. Marangoni, B. Gayet, M. Pocard, I. Bieche, M.-F. Poupon, D. Bellet, V. Dangles-Marie, Newly characterised ex vivo colospheres as a three-dimensional colon cancer cell model of tumour aggressiveness, *Br. J. Cancer.* 101 (2009) 473–482. doi:10.1038/sj.bjc.6605173.
- [19] L.B. Weiswald, D. Bellet, V. Dangles-Marie, Spherical cancer models in tumor biology, *Neoplasia.* 17 (2015) 1–15. doi:10.1016/j.neo.2014.12.004.
- [20] F. Pampaloni, E.G. Reynaud, E.H.K. Stelzer, The third dimension bridges the gap between cell culture and live tissue, *Nat. Rev. Mol. Cell Biol.* 8 (2007) 839–845. doi:10.1038/nrm2236.
- [21] Y.-C. Chen, X. Lou, Z. Zhang, P. Ingram, E. Yoon, High-Throughput Cancer Cell Sphere Formation for Characterizing the Efficacy of Photo Dynamic Therapy in 3D Cell Cultures, *Sci. Rep.* 5 (2015) 12175. doi:10.1038/srep12175.
- [22] F. Hirschhaeuser, H. Menne, C. Dittfeld, J. West, W. Mueller-Klieser, L.A. Kunz-Schughart, Multicellular tumor spheroids: An underestimated tool is catching up again, *J. Biotechnol.* 148 (2010) 3–15. doi:10.1016/j.jbiotec.2010.01.012.
- [23] S. Breslin, L. O'Driscoll, Three-dimensional cell culture: The missing link in drug discovery, *Drug Discov. Today.* 18 (2013) 240–249. doi:10.1016/j.drudis.2012.10.003.
- [24] O.J. Klein, B. Bhayana, Y.J. Park, C.L. Evans, In vitro optimization of EtNBS-PDT against hypoxic tumor environments with a tiered, high-content, 3D model optical screening platform, *Mol. Pharm.* 9 (2012) 3171–3182. doi:10.1021/mp300262x.
- [25] B. Gustavsson, G. Carlsson, D. MacHover, N. Petrelli, A. Roth, H.J. Schmoll, K.M. Tveit, F. Gibson, A review of the evolution of systemic chemotherapy in the management of colorectal cancer, *Clin. Colorectal Cancer.* 14 (2015) 1–10. doi:10.1016/j.clcc.2014.11.002.
- [26] M.S. Edwards, S.D. Chadda, Z. Zhao, B.L. Barber, D.P. Sykes, A systematic review of treatment

- guidelines for metastatic colorectal cancer, *Color. Dis.* 14 (2012) 31–47. doi:10.1111/j.1463-1318.2011.02765.x.
- [27] K.C. Chen, Y.S. Hsieh, Y.F. Tseng, M.J. Shieh, J.S. Chen, H.S. Lai, J.M. Lee, Pleural photodynamic therapy and surgery in lung cancer and thymoma patients with pleural spread, *PLoS One.* 10 (2015) 1–7. doi:10.1371/journal.pone.0133230.
- [28] E. V Filonenko, A.D. Kaprin, B.Y. a. Alekseev, O.I. Apolikhin, E.K. Slovokhodov, V.I. Ivanova-Radkevich, A.N. Urlova, 5-Aminolevulinic acid in intraoperative photodynamic therapy of bladder cancer (results of multicenter trial), *Photodiagnosis Photodyn. Ther.* 16 (2016) 106–109. doi:http://dx.doi.org/10.1016/j.pdpdt.2016.09.009.
- [29] K. Moghissi, K. Dixon, S. Gibbins, A Surgical View of Photodynamic Therapy in Oncology: A Review, *Surg. J.* 01 (2015) e1–e15. doi:10.1055/s-0035-1565246.
- [30] D. van Straten, V. Mashayekhi, H. de Bruijn, S. Oliveira, D. Robinson, Oncologic Photodynamic Therapy: Basic Principles, Current Clinical Status and Future Directions, *Cancers (Basel).* 9 (2017) 19. doi:10.3390/cancers9020019.
- [31] S.I. Moriwaki, J. Misawa, Y. Yoshinari, I. Yamada, M. Takigawa, Y. Tokura, Analysis of photosensitivity in Japanese cancer-bearing patients receiving photodynamic therapy with porfimer sodium (Photofrin)., *Photodermatol. Photoimmunol. Photomed.* 17 (2001) 241–3. doi:DOI 10.1034/j.1600-0781.2001.170507.x.
- [32] S.J. Madsen, C.H. Sim, B.J. Tromberg, V. Cristini, N. De Magalhães, H. Hirschberg, Multicell tumor spheroids in photodynamic therapy, *Lasers Surg. Med.* 38 (2006) 555–564. doi:10.1002/lsm.20350.
- [33] G. Mehta, A.Y. Hsiao, M. Ingram, G.D. Luker, S. Takayama, Opportunities and challenges for use of tumor spheroids as models to test drug delivery and efficacy, *J. Control. Release.* 164 (2012) 192–204. doi:10.1016/j.jconrel.2012.04.045.
- [34] A.A.R. Kamuhabwa, A. Huygens, P.A.M. De Witte, Photodynamic therapy of transitional cell carcinoma multicellular tumor spheroids with hypericin., *Int. J. Oncol.* 23 (2003) 1445–1450.
- [35] Y. Yang, X. Yang, J. Zou, C. Jia, Y. Hu, H. Du, H. Wang, Evaluation of photodynamic therapy efficiency using an in vitro three-dimensional microfluidic breast cancer tissue model, *Lab a Chip - Miniaturisation Chem. Biol.* 15 (2015) 735–744. doi:10.1039/c4lc01065e.

- [36] W. Mo, J. Zhang, Review Article Human ABCG2 : structure , function , and its role in multidrug resistance, *Int. J. Biochem. Mol. Biol.* 3 (2012) 1–27.
- [37] M. Galetti, P.G. Petronini, C. Fumarola, D. Cretella, S. La Monica, M. Bonelli, A. Cavazzoni, F. Saccani, C. Caffarra, R. Andreoli, A. Mutti, M. Tiseo, A. Ardizzoni, R.R. Alfieri, Effect of ABCG2/BCRP expression on efflux and uptake of Gefitinib in NSCLC cell lines, *PLoS One*. 10 (2015) 1–18. doi:10.1371/journal.pone.0141795.
- [38] K. Noguchi, K. Katayama, Y. Sugimoto, Human ABC transporter ABCG2/BCRP expression in chemoresistance: basic and clinical perspectives for molecular cancer therapeutics., *Pharmgenomics. Pers. Med.* 7 (2014) 53–64. doi:10.2147/PGPM.S38295.
- [39] J. Liao, F. Qian, N. Tchabo, P. Mhaweche-Fauceglia, A. Beck, Z. Qian, X. Wang, W.J. Huss, S.B. Lele, C.D. Morrison, K. Odunsi, Ovarian cancer spheroid cells with stem cell-like properties contribute to tumor generation, metastasis and chemotherapy resistance through hypoxia-resistant metabolism, *PLoS One*. 9 (2014) 1–13. doi:10.1371/journal.pone.0084941.
- [40] H.G. Liu, Y.F. Pan, J. You, O.C. Wang, K. Te Huang, X.H. Zhang, Expression of ABCG2 and its significance in colorectal cancer, *Asian Pacific J. Cancer Prev.* 11 (2010) 845–848.
- [41] J.H. Kim, J.M. Park, Y.J. Roh, I.-W. Kim, T. Hasan, M.-G. Choi, Enhanced efficacy of photodynamic therapy by inhibiting ABCG2 in colon cancers, *BMC Cancer*. 15 (2015) 504. doi:10.1186/s12885-015-1514-4.
- [42] J. Morgan, J.D. Jackson, X. Zheng, S.K. Pandey, R.K. Pandey, Substrate Affinity of Photosensitizers Derived from Chlorophyll-a: The ABCG2 Transporter Affects the Phototoxic Response of Side Population Stem Cell-like Cancer Cells to Photodynamic Therapy, *Mol. Pharm.* 7 (2010) 1789–1804. doi:10.1021/mp100154j.
- [43] T. Ishikawa, Y. Kajimoto, W. Sun, H. Nakagawa, Y. Inoue, Y. Ikegami, S.I. Miyatake, T. Kuroiwa, Role of Nrf2 in cancer photodynamic therapy: Regulation of human ABC transporter ABCG2, *J. Pharm. Sci.* 102 (2013) 3058–3069. doi:10.1002/jps.23563.
- [44] R. Jendzelovsky, J. Mikes, J. Koval, K. Soucek, J. Prochazkova, M. Kello, V. Sackova, J. Hofmanova, A. Kozubik, P. Fedorocko, R. Jendzelovský, J. Mikes, J. Koval', K. Soucek, J. Procházková, M. Kello, V. Sacková, J. Hofmanová, A. Kozubík, P. Fedorocko, Drug efflux transporters, MRP1 and BCRP,

- affect the outcome of hypericin-mediated photodynamic therapy in HT-29 adenocarcinoma cells, *Photochem. Photobiol. Sci.* 8 (2009) 1716–1723. doi:10.1039/b9pp00086k.
- [45] M. Šemeláková, R. Jendželovský, P. Fedorocko, Drug membrane transporters and CYP3A4 are affected by hypericin, hyperforin or aristoforin in colon adenocarcinoma cells, *Biomed. Pharmacother.* 81 (2016) 38–47. doi:10.1016/j.biopha.2016.03.045.
- [46] S. Shen, D. Callaghan, C. Juzwik, H. Xiong, P. Huang, W. Zhang, ABCG2 reduces ROS-mediated toxicity and inflammation: A potential role in Alzheimer's disease, *J. Neurochem.* 114 (2010) 1590–1604. doi:10.1111/j.1471-4159.2010.06887.x.
- [47] A.G. Poleshko, I.D. Volotovskii, The role of ABCG2 in maintaining the viability and proliferative activity of bone marrow mesenchymal stem cells in hypoxia, *Biophysics (Oxf.)* 61 (2016) 271–276. doi:10.1134/S0006350916020159.
- [48] G.A. Barron, H. Moseley, J.A. Woods, Differential sensitivity in cell lines to photodynamic therapy in combination with ABCG2 inhibition, *J. Photochem. Photobiol. B Biol.* 126 (2013) 87–96. doi:10.1016/j.jphotobiol.2013.07.003.
- [49] P. Palasuberniam, X. Yang, D. Kraus, P. Jones, K.A. Myers, B. Chen, ABCG2 transporter inhibitor restores the sensitivity of triple negative breast cancer cells to aminolevulinic acid-mediated photodynamic therapy., *Sci. Rep.* 5 (2015) 13298. doi:10.1038/srep13298.
- [50] S.A. Abdel Gaber, P. Müller, W. Zimmermann, D. Hüttenberger, R. Wittig, M.H. Abdel Kader, H. Stepp, ABCG2-mediated suppression of chlorin e6 accumulation and photodynamic therapy efficiency in glioblastoma cell lines can be reversed by KO143, *J. Photochem. Photobiol. B Biol.* 178 (2018) 182–191. doi:10.1016/j.jphotobiol.2017.10.035.
- [51] L.C. Kimlin, G. Casagrande, V.M. Virador, In vitro three-dimensional (3D) models in cancer research: An update, *Mol. Carcinog.* 52 (2013) 167–182. doi:10.1002/mc.21844.
- [52] L.M. Langan, N.J.F. Dodd, S.F. Owen, W.M. Purcell, S.K. Jackson, A.N. Jha, Correction: Direct measurements of oxygen gradients in spheroid culture system using electron paramagnetic resonance oximetry, *PLoS One.* 11 (2016) 1–13. doi:10.1371/journal.pone.0160795.
- [53] H.S. De Bruijn, S. Brooks, A. Van Der Ploeg-Van Den Heuvel, T.L.M. Ten Hagen, E.R.M. De Haas, D.J. Robinson, Light fractionation significantly increases the efficacy of photodynamic therapy using

BF-200 ALA in normal mouse skin, PLoS One. 11 (2016) 1–20. doi:10.1371/journal.pone.0148850.

- [54] H.S. De Bruijn, A.G. Casas, G. Di Venosa, L. Gandara, H.J.C.M. Sterenberg, A. Batlle, D.J. Robinson, Light fractionated ALA-PDT enhances therapeutic efficacy in vitro; The influence of PpIX concentration and illumination parameters, Photochem. Photobiol. Sci. 12 (2013) 241–245. doi:10.1039/c2pp25287b.

FIGURES

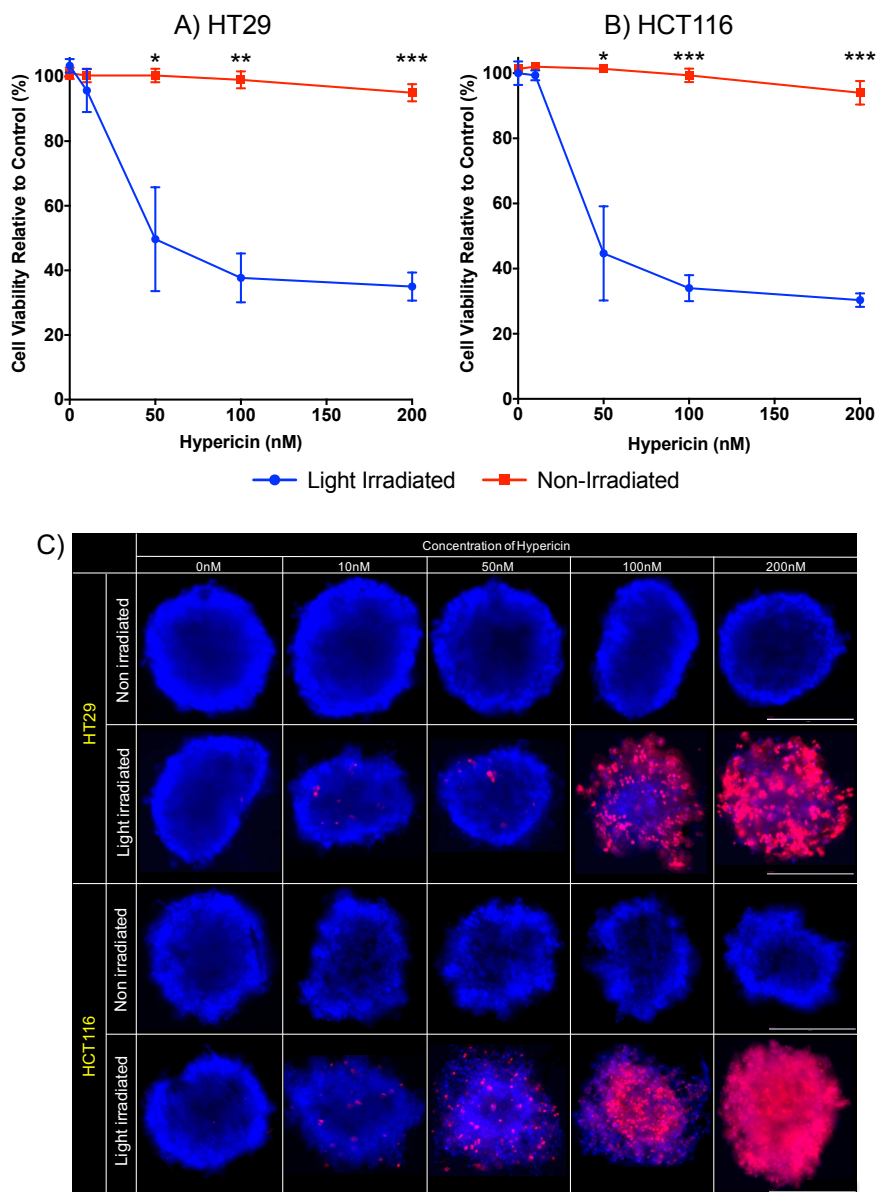


Figure 1. Light dependant cytotoxicity of Hypericin **A)** HT29 and **B)** HCT116 2D cultures were incubated with varying concentrations of Hypericin and then irradiated with light or kept in the dark. After 24 hours, cell viability was assessed by staining cultures with Propidium Iodide and quantifying fluorescence. **C)** HT29 and HCT116 spheroids were treated with varying concentrations of Hypericin +/- light. Spheroids were then stained with Hoechst 33342 (blue fluorescence) and Propidium Iodide (red fluorescence) and then imaged. Scalebar = 400µm. Data are shown relative to control treated cells and represent means with SD of 3 independent experiments. * $p < 0.01$, ** $p < 0.001$, *** $p < 0.0001$.

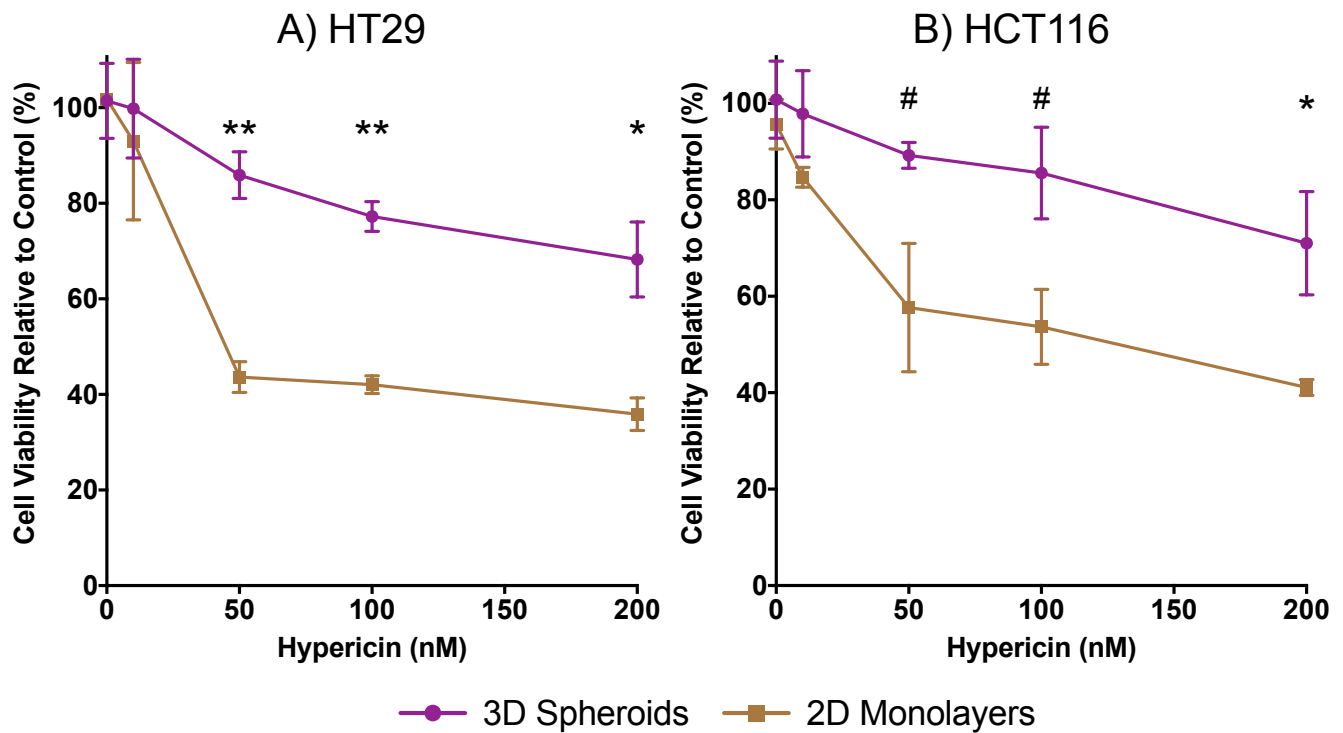


Figure 2. Comparison between 2D and spheroid CRC cell models in response to Hypericin-PDT. A) HT29 and B) HCT116 2D and spheroid models were incubated with varying concentrations of Hypericin and then irradiated with light. After 24 hours, cultures were stained with Propidium Iodide and fluorescence was quantified. Data are shown relative to control treated cultures and represent means with SD of 3 independent experiments. # $p < 0.05$, * $p < 0.01$, ** $p < 0.001$.

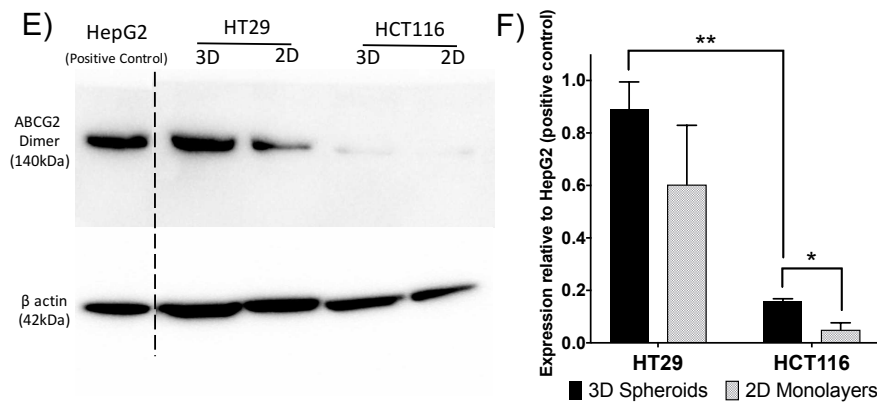
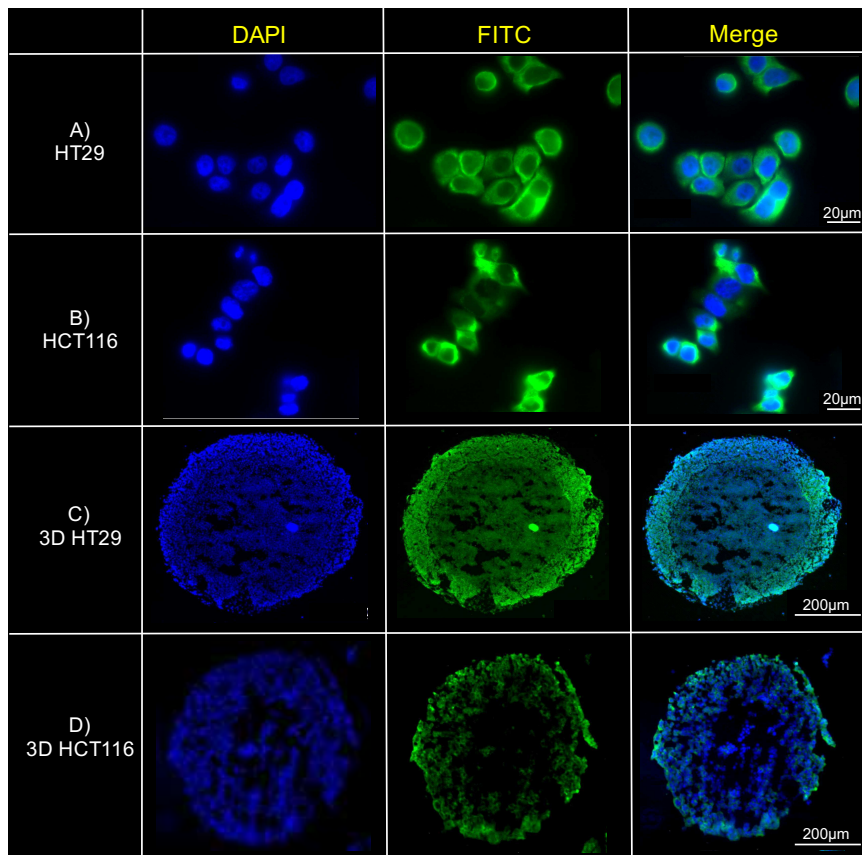


Figure 3. Expression of ABCG2 protein in 2D and spheroid CRC cell models. A) 2D HT29 B) 2D HCT116 C) HT29 spheroid sections and D) HCT116 spheroid sections were fixed and incubated with a primary anti-BCRP (ABCG2) and secondary Alexa Fluor 488 antibody (Green) and mounted with DAPI (Blue). E) Western blot analysis of ABCG2 in protein extracts from 3D spheroid and 2D models of HT29 and HCT116 (HepG2 cell lysates served as positive control). F) Quantitative analysis of western blots. Data are shown relative to the protein expression of ABCG2 in HepG2 lysates and represent means with SD of 3 independent experiments. * $p < 0.01$, ** $p < 0.001$.

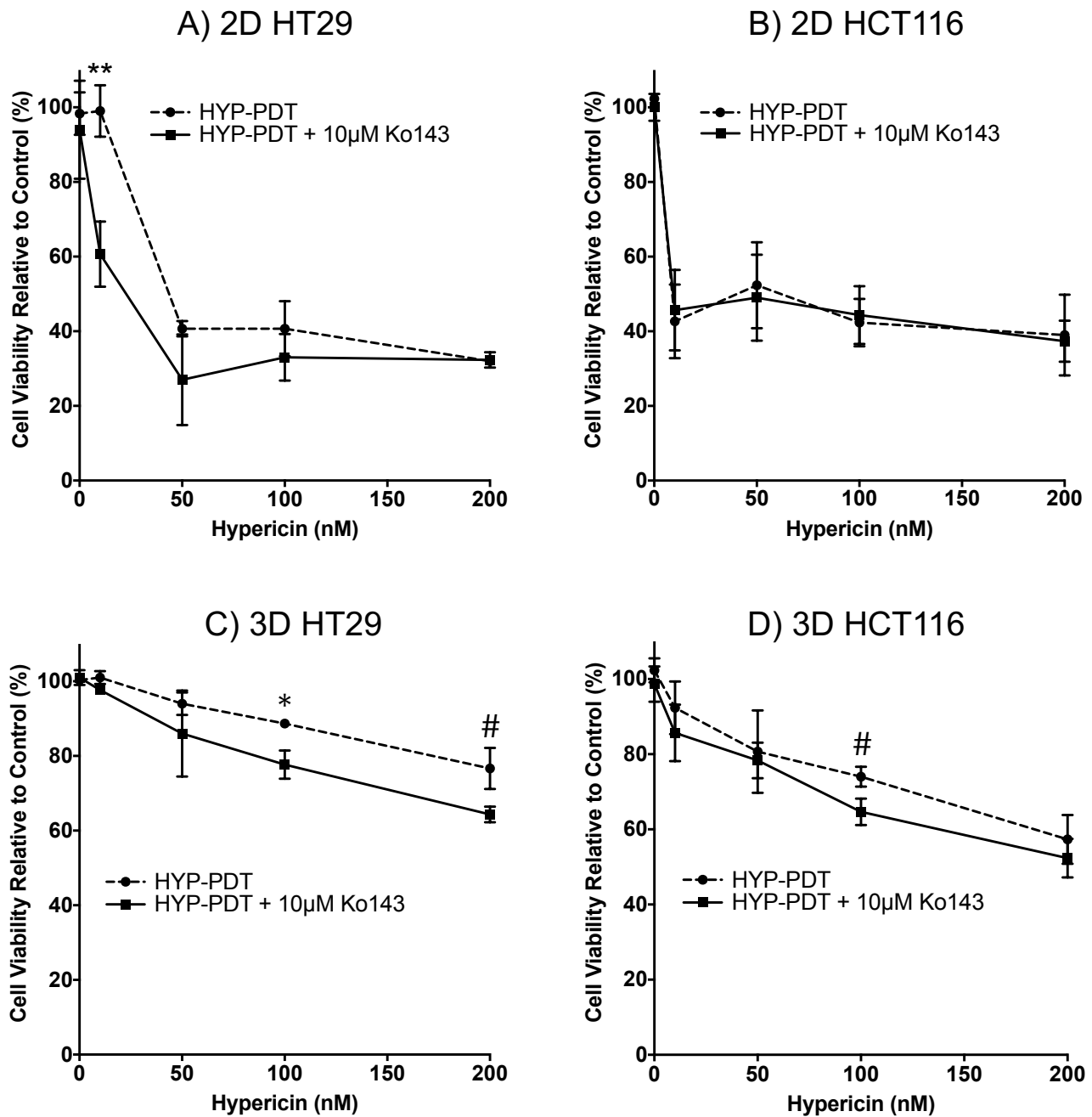


Figure 4. Co-treating 2D and spheroid CRC cell models with Ko143 and Hypericin-PDT (HYP-PDT) A) 2D HT29 B) 2D HCT116 C) HT29 spheroid and D) HCT116 spheroid cultures were co-treated with varying concentrations of Hypericin and 10µM Ko143 or Hypericin alone and then irradiated with light. After 24 hours, cultures were stained with Propidium Iodide and fluorescence was quantified. Data are shown relative to control treated cultures and represent means with SD of 3 independent experiments. # $p < 0.05$, * $p < 0.01$, ** $p < 0.005$.

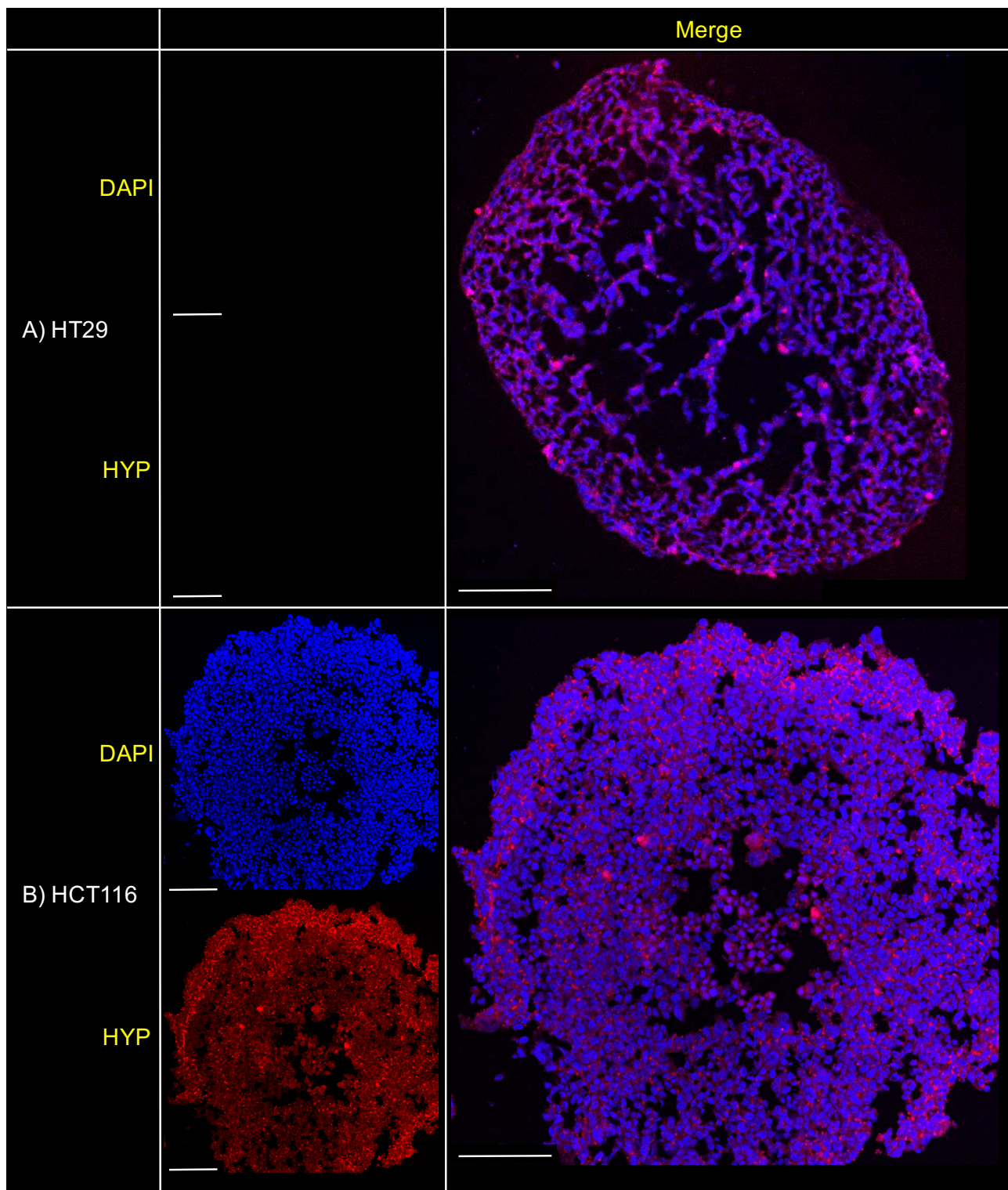


Figure 5. Penetration of Hypericin through CRC spheroid cultures. A) HT29 and B) HCT116 spheroids were incubated with Hypericin (HYP, Red) for 16 hours. Spheroids were then sectioned, mounted with DAPI (Blue) and fluorescently imaged. Scalebar = 100 μ m.

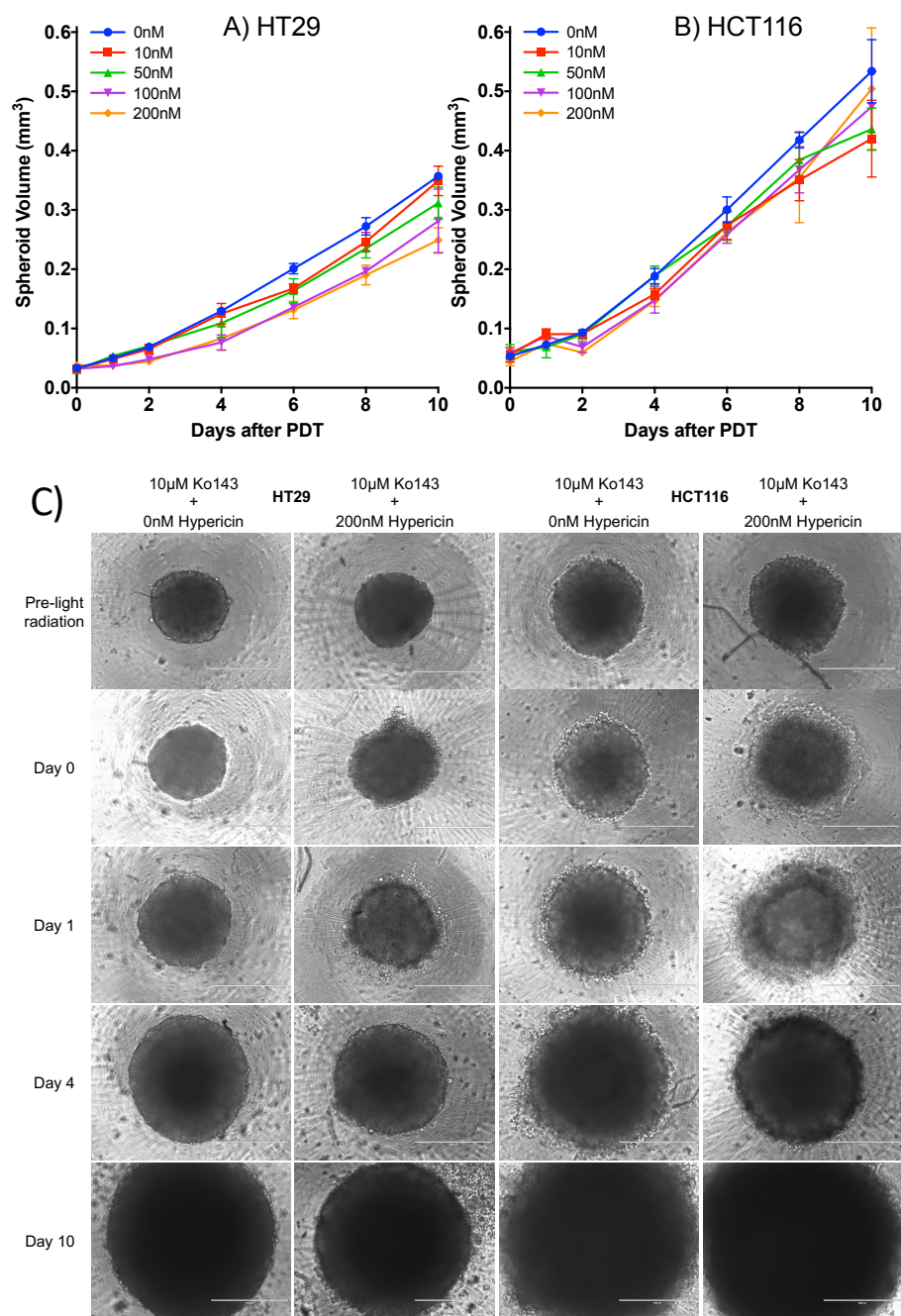


Figure 6. Long-term culture of spheroids following Ko143 and Hypericin-PDT co-treatment

A) HT29 and **B)** HCT116 spheroids were incubated with varying concentrations of Hypericin and 10 μ M Ko143 and then irradiated with light. Volumes of spheroids were measured for 10 days following light radiation. **C)** Images of 10 μ M Ko143 treated only and 10 μ M Ko143 and 200nM Hypericin co-treated HT29 and HCT116 spheroids pre-light radiation and at days 0, 1, 4 and 10 following light irradiation. Scalebar = 400 μ m. Data shown represents means with SD of 3 independent experiments.